Radio-frequency characteristics of graphene oxide

Whan Kyun Kim,[1] Young Mo Jung,[1] Joon Hyong Cho,[1] Ji Yoong Kang,[1] Ju Yeong Oh,[1] Hosung Kang,[2] Hee-Jo Lee,[3] Jae Hun Kim,[4] Seok Lee,[4] H. J. Shin,[5] J. Y. Choi,[5] S. Y. Lee,[5] Y. C. Kim,[5] I. T. Han,[5] J. M. Kim,[5] Jong-Gwan Yook,[3] Seunghyun Baik,[2] and Seong Chan Jun[1,a)]

[1]*School of Mechanical Engineering, Yonsei University, Seoul 120-749, Republic of Korea*
[2]*Department of Energy Science, School of Mechanical Engineering, SKKU Advanced Institute of Nanotechnology, Sungkyunkwan University, Suwon 440-746, Republic of Korea*
[3]*School of Electrical and Electronic Engineering, Yonsei University, Seoul 120-749, Republic of Korea*
[4]*Korea Institute of Science and Technology, Seoul 130-650, Republic of Korea*
[5]*Samsung Advanced Institute of Technology, Yongin, Gyeonggi-Do 446-712, Republic of Korea*

(Received 6 May 2010; accepted 28 September 2010; published online 9 November 2010)

We confirm graphene oxide, a two-dimensional carbon structure at the nanoscale level can be a strong candidate for high-efficient interconnector in radio-frequency range. In this paper, we investigate high frequency characteristics of graphene oxide in range of 0.5–40 GHz. Radio-frequency transmission properties were extracted as S-parameters to determine the intrinsic ac transmission of graphene sheets, such as the impedance variation dependence on frequency. The impedance and resistance of graphene sheets drastically decrease as frequency increases. This result confirms graphene oxide has high potential for transmitting signals at gigahertz ranges. © *2010 American Institute of Physics*. [doi:10.1063/1.3506468]

Graphene, a single sheet of carbon, is composed of a hexagonal two-dimensional network of carbon atoms, which presents exotic electronic properties. Graphene is quite stable and inert and, as such, can be used over large areas with low defect densities,[1] low electron-phonon scattering rates,[2] and very high carrier mobilities.[3] Graphene can also be gated for use as a channel in transistors or as an interconnect.[4]

Graphene is generally obtained from highly oriented pyrolytic graphite by mechanical cleavage.[5,6] Even though uniform graphene can be extracted, there exist many disadvantages, such as laborious effort to find suitable samples, and difficulty to locate graphene at particular positions. To overcome these problems, graphene oxide (GO), consisting of hydrophilic oxygenated graphene sheets could be an alternate method for carbon or nanoscale electronics and substitute for complementary metal-oxide semiconductor circuits. Recent researches include the electrical properties dependent on gate voltage,[7] temperature-dependent electrical conductivity[8] and molecular sensor applications.[9] This is high-yield production method and positioning at desired locations for graphene-based circuits compared with micromechanical cleavage method. We report electronic transport studies of individual multiple-layer GO in radio-frequency range, and confirm the superiority of carbon's signal propagation among nano-micro electronic materials.

GO sheets, synthesized from SP-1 graphite powder by a modified Hummers method,[10,11] were dispersed in dimethylformamide (Aldrich, anhydrous, 99.8%) at a mass ratio of 0.0001 by sonicating at 135 W for 10 min. In the next step, a few layers of GO sheets were dielectrophoretically deposited on the electrodes.[11,12] A drop of the suspension (0.5 μl) was placed onto the electrodes, and an alternating current electric field (Agilent, 33220 A, 10 V_{pp}, 100 kHz) was applied for 1 min. The droplet was blown off using nitrogen gas (99.8% purity), and the electric field was switched off. Finally, the deposited GO sheets were thermally reduced in argon (800 mm Hg) to restore electrical conductivity.[11] The temperature was ramped to 400 °C (1 °C/min), maintained for 2 h, and then allowed to cool to room temperature.

Frequency-dependent microwave transmission could be observed from 0.5 to 40 GHz via two-port measurement. From the measured S-parameters, ac transmission parameters that depend on frequency were extracted. The thickness of SiO_2 film was 500 nm in order to reduce the substrate loss, which is one of the main signal losses in high-frequency nanoelectric device measurements. In order to observe the ac transmission properties of graphene sheets, we fabricated devices compatible with ground-signal-ground (GSG) probing. Figure 1(a) shows a schematic view of our devices. The electrodes were patterned by photolithography. The electrodes made of Cr/Au (10/400 nm) are deposited on the SiO_2 substrate using e-beam evaporation. Identical pad structures

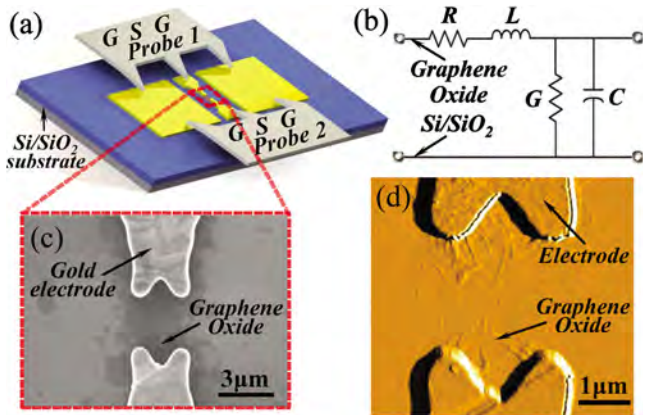

FIG. 1. (Color online) Devices for radio-frequency measurements. (a) A structure for GSG measurements. (b) The equivalent circuit model of GO interconnect. (c) SEM images of GO sheets between the electrodes which have the gap sizes of 3 μm. (d) The AFM image of GO sheets used in the experiment.

a)Electronic mail: scj@yonsei.ac.kr.

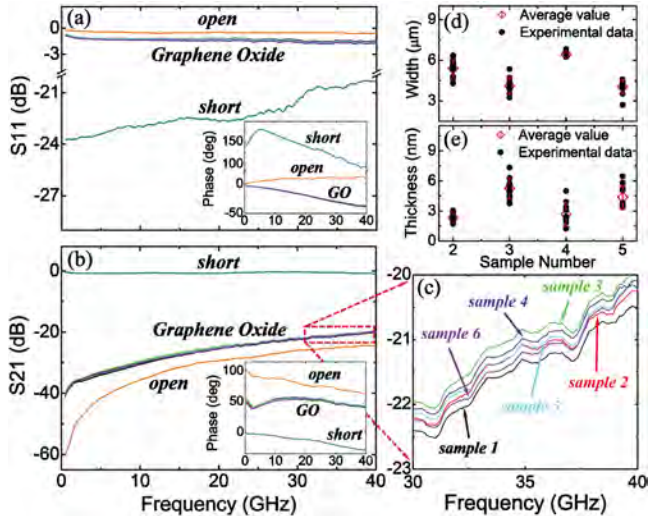

FIG. 2. (Color online) Measured S-parameter data. (a) Reflected S-parameter, S11 magnitude: open, GO sheets, and short sample, in the order of decreasing magnitude. The inset is S11 phase data of measured samples. (b) Transmitted S-parameter, S21 magnitude: short, GO sheets, and open sample, in the order of decreasing magnitude. The inset is S21 phase data of measured samples. (c) S21 magnitude of the samples from 30 to 40 GHz decreases as the order of sample 3–4–5–2–6–1. (d) The width and (e) thickness of graphene sheets within samples. Ten points (black) are measured at regular intervals in each sample. The error bar shows the standard deviation of measured data.

without graphene sheets ("open"), and with a rectangular Au wire of 3 μm in width ("short"), respectively, were also measured. High frequency properties of GO as well as the substrate effects were extracted by the equivalent circuit model as shown in Fig. 1(b). The transmission line is decomposed into distributed elements, such as R, L, G, and C which are series resistance, inductance, shunt conductance, and shunt capacitance per unit length. Figure 1(c) shows a close-up view of the scanning electron microscope (SEM) image of our device sample, and the thickness of graphene sheets used in the experiment was measured using an atomic force microscope (AFM) in Fig. 1(d). The high frequency transmission of GO is majorly dominated by geometry effects, chemical treatment, and annealing.

In our study, six samples, extracted from a number of samples with different gap sizes, were analyzed. The effective graphene sheet lengths (i.e., the gap between the IN and OUT electrodes) are 8.5 μm for sample 1, 3 μm for sample 2, 2.8 μm for sample 3, 2.2 μm for sample 4, and 2.4 μm for sample 5, and 4.3 μm for sample 6. S-parameters for six samples were measured using the Agilent E8364A network analyzer at −20 dBm. Figures 2(a) and 2(b) show the measured S-parameter data. S_{11} magnitude plots of GO decrease as shown in Fig. 2(a), and reversely S_{21} plots increase in Fig. 2(b) as the frequency increases. It can be seen that all of the samples with graphene sheets transmit higher current than the open sample. In the plots of graphene sheets, magnitudes at 30–40 GHz decrease in the following sample order: 3, 4, 5, 2, 6, and 1. These results indicate that the parasitic capacitive effect influences the S_{21} magnitudes of samples 3, 4, 5, and 2 more strongly because their gap sizes are smaller than those of samples 6 and 1. Figure 2(b) shows that the differences in S_{21} magnitude between graphene sheets and the open sample are 11–12 dB at 3 GHz and approximately 4.5 dB at 40 GHz, which indicates that the parasitic capacitive effect dominates with increasing frequency. The averaged S_{21} magnitude of graphene sheet samples at 40 GHz (−19.9 dB) is nearly 4 dB higher than the multiwalled nanotubes bundles (−23.6 dB at 40 GHz)[13] and 7 dB higher than the single wall carbon nanotubes (−27 dB at 40 GHz)[14] reported previously.

Figure 2(c) shows transmission capabilities of the measured samples from 30 to 40 GHz. We considered the geometries of graphene sheets to effectively analyze electrical properties within samples; the widths and thicknesses of GO sheets were presented, as shown in Figs. 2(d) and 2(e). Root mean square roughness values measured by AFM are 3.7 ± 0.5 nm for sample 2, 6.8 ± 0.3 nm for sample 3, 3.4 ± 0.4 nm for sample 4, and 2.4 ± 0.2 nm for sample 5 in the area of 8 μm^2. Although graphene sheets have an erratic shape, since thickness and width were measured at the regular intervals to utilize the average values and the standard deviation, the relative resistance dependent on the geometries of the samples was briefly determined. The resistance of the transmission line with width w and thickness t is shown as $R=\rho L/wt$, where ρ and L are the resistivity and the effective length of GO sheets, respectively.[15] The resistivity of GO is 3.5×10^{-4} Ω m.[11] The average widths of samples 2, 3, 4, and 5 are 5.41 μm, 4.11 μm, 6.42 μm, and 4.03 μm, respectively. The average thicknesses of those are 2.33 μm, 5.27 μm, 2.65 μm, and 4.38 μm, respectively. The resistances of transmission lines accordingly increase in the following sample order—3 (45.25 Ω), 4 (46.42 Ω), 5 (47.59 Ω), 2 (83.30 Ω)—which roughly corresponds to the measured S_{21} magnitudes of Fig. 2(c). Sample 3 has the smallest resistance, even though it shows the largest roughness value. Therefore, transmission properties of GO are dominated by average values of geometries than roughness of it.

A Y-parameter de-embedding technique was used in order to eliminate the parasitic capacitive effect of electrodes from the measured data.[16] The de-embedding procedure is carried out using $[Y_{int}]=[Y_{meas}]-[Y_{open}]$, where $[Y_{int}]$ are the Y-parameters of the intrinsic interconnect, $[Y_{meas}]$ and $[Y_{open}]$ are the measured Y-parameters obtained by S-parameters of the samples with GO sheets and open sample.

Figure 3(a) shows the real and imaginary parts of the characteristic impedance of the graphene sheets, Au wire which has 3 μm in width and 10 nm in thickness, and open structure. The impedance within pad structures decreases as the following order: open, Au wire, and GO. The averaged real parts of the impedance monotonically decrease from 450 Ω at 0.5 GHz to 19 Ω at 40 GHz. (Au wire: 1445 Ω at 0.5 GHz to 154 Ω at 40 GHz, open: 1984 Ω at 0.5 GHz to 158 Ω at 40 GHz) The interconnect characteristic impedance, Z, can be separated into real and imaginary parts by squaring it; $Z^2=\{(RG+\omega^2LC)/[G^2+(\omega C)^2]\}+j\{(\omega LC-\omega RC)/[G^2+(\omega C)^2]\}$. The imaginary part of the impedance is always negative over the entire frequency range, which means that the interconnect reactance of graphene sheets is capacitive.

With the two-port S-parameter data, relative power lost from traveling microwaves is given by $\text{Loss}=1-(|S_{11}|^2+|S_{21}|^2)$. The loss represents the difference between the normalized input power and the reflected or transmitted output power. In Fig. 3(b), all of the samples measured show rapidly

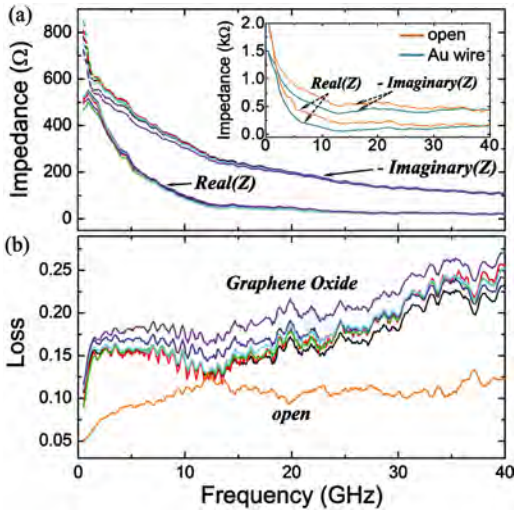

FIG. 3. (Color online) (a) Real and imaginary parts of the characteristic impedance of GO sheets, open, and Au wire (inset). (b) The signal loss with respect to frequency: GO sheets, and open sample, in the order of decreasing magnitude.

increasing loss up to about 1.5 GHz, after certain point the loss remains almost constant until 20 GHz, and then the power loss of the graphene sheets increases again. The loss significantly increases above 20 GHz due to the large coupling generated by electric fields surrounding the transmission line and electrodes.[17]

To obtain transmission line parameters, such as R, L, G, and C,[18] the relationships between the propagation constant, γ and the characteristic impedances, Z, R, L, G, and C, were utilized via $\gamma=\sqrt{(R+j\omega L)(G+j\omega C)}$, $Z=\sqrt{(R+j\omega L)/(G+j\omega C)}$.

Figures 4(a)–4(d) show R, L, G, and C, which were extracted by combining these equations. As seen in Fig. 4(a), the averaged resistance of the samples drastically decreases from 550 Ω/μm at 0.5 GHz to 77 Ω/μm at 15 GHz and then gradually decreases to 11 Ω/μm at 40 GHz. (Au wire: 1647 to 60 Ω/μm, open: 4278 to 407 Ω/μm) Figure 4(b) shows that the average series inductance decreases from 0.27 μH/μm at 0.5 GHz to 0.4 nH/μm at 40 GHz. (Au wire: 1.06 to 0.9 nH/μm, open: 0.32 to 0.7 nH/μm) In Fig. 4(c), the shunt conductance that represents dielectric loss increases from 0.55 to 2.5 mS/μm. (Au wire: 0.39 to

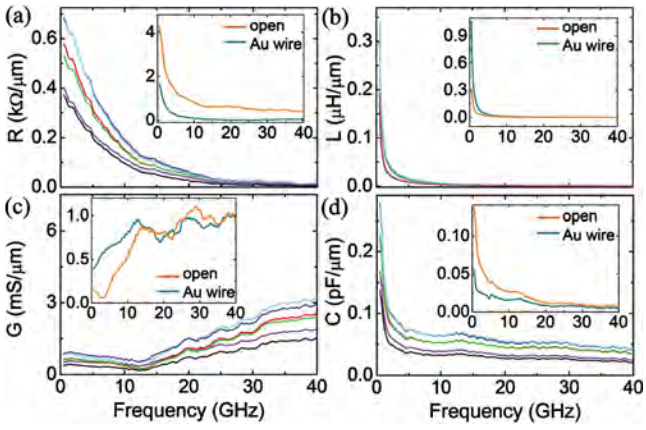

FIG. 4. (Color online) Extracted transmission line parameters of graphene sheets, open, and Au wire (inset). (a) R: resistance, (b) L: inductance, (c) G: the shunt conductance, (d) C: the shunt capacitance.

0.97 mS/μm, open: 0.14 to 0.92 mS/μm) The induced eddy current in the graphene sheet interconnector and eddy currents in the silicon substrate cause the series inductance to decrease.[19] In addition, the shunt conductance that increases roughly proportionally to frequency is affected by the eddy currents at high frequency. Figure 4(d) shows that the shunt capacitance drastically decreases from 0.21 to 0.036 pF/μm, whereas it remains almost constant from 10 GHz to 40 GHz. (Au wire: 55 to 5.4 fF/μm, open: 136 to 7.66 fF/μm)

This paper discusses high-frequency properties of graphene sheets originating from GO. Although signal loss slightly increase with increasing frequency, the impedance and series resistance extracted from the S-parameter of GO sheets may sharply decrease as the frequency increases. GO can be easily fabricated at the desired position and has very efficient microwave transmission capability. Therefore, we expect that GO could be used for transmission lines in next-stage electronics and could be very strong candidate for nanocarbon electronics. There remain many issues such as theoretical approaches for transmission mechanism of graphene, contact effects for transmission, and defects in graphene surface for future study of GO sheets.

This work was partially supported by the Priority Research Centers Program (Grant No. 2009-0093823), the Pioneer Research Center Program (Grant No. 2010-0019313), and Basic Science Research Program (Grant No. 2010-8-0874) through the National Research Foundation of Korea (NRF) funded by the Ministry of Education, Science and Technology (MEST) of the Korean government. We thank R. S. Ruoff and S. Stankovich for providing the GO used in this study.

[1] J. Coraux, A. T. N'Diaye, C. Busse, and T. Michely, Nano Lett. **8**, 565 (2008).
[2] S. V. Morozov, K. S. Novoselov, M. I. Katsnelson, F. Schedin, D. C. Elias, J. A. Jaszczak, and A. K. Geim, Phys. Rev. Lett. **100**, 016602 (2008).
[3] Y. Zhang, J. W. Tan, H. L. Stormer, and P. Kim, Nature (London) **438**, 201 (2005).
[4] K. S. Novoselov, A. K. Geim, S. V. Morozov, D. Jiang, Y. Zhang, S. V. Dubonos, I. V. Grigorieva, and A. A. Firsov, Science **306**, 666 (2004).
[5] K. S. Novoselov, D. Jiang, F. Schedin, T. J. Booth, V. V. Khotkevich, S. V. Morozov, and A. K. Geim, Proc. Natl. Acad. Sci. U.S.A. **102**, 10451 (2005).
[6] A. K. Geim and K. S. Novoselov, Nature Mater. **6**, 183 (2007).
[7] I. Jung, D. A. Dikin, R. D. Piner, and R. S. Ruoff, Nano Lett. **8**, 4283 (2008).
[8] C. Gómez-Navarro, R. T. Weitz, A. M. Bittner, M. Scolari, A. Mews, M. Burghard, and K. Kern, Nano Lett. **7**, 3499 (2007).
[9] J. T. Robinson, F. K. Perkins, E. S. Snow, Z. Wei, and P. E. Sheehan, Nano Lett. **8**, 3137 (2008).
[10] W. Hummers and R. Offeman, J. Am. Chem. Soc. **80**, 1339 (1958).
[11] H. Kang, A. Kulkarni, S. Stankovich, R. S. Ruoff, and S. Baik, Carbon **47**, 1520 (2009).
[12] S. Hong, S. Jung, S. Kang, Y. Kim, X. Chen, S. Stankovich, R. S. Ruoff, and S. Baik, J. Nanosci. Nanotechnol. **8**, 424 (2008).
[13] A. Tselev, M. Woodson, C. Qian, and J. Liu, Nano Lett. **8**, 152 (2008).
[14] J. J. Plombon, K. P. O'Brien, F. Gstrein, V. M. Dubin, and Y. Jiao, Appl. Phys. Lett. **90**, 063106 (2007).
[15] W. Steinhögl, G. Schindler, G. Steinlesberger, M. Traving, and M. Engelhardt, J. Appl. Phys. **97**, 023706 (2005).
[16] J.-M. Bethoux, H. Happy, G. Dambrine, V. Derycke, M. Goffman, and J.-P. Bourgoin, IEEE Electron Device Lett. **27**, 681 (2006).
[17] B. Kleveland, C. H. Diaz, D. Vook, L. Madden, T. H. Lee, and S. S. Wong, IEEE J. Solid-State Circuits **36**, 1480 (2001).
[18] D. M. Pozar, *Microwave Engineering* (Wiley, New York, 2005).
[19] B. Kleveland, X. Qi, L. Madden, T. Furusawa, R. W. Dutton, M. A. Horowitz, and S. S. Wong, IEEE J. Solid-State Circuits **37**, 716 (2002).